Conductive Microbead Detection by Helmholtz Coil Technique With SV-GMR Sensor

Conductive Microbead Detection by Helmholtz Coil Technique With SV-GMR Sensor

T.Somsak[1], K.Chomsuwan[1], S.Yamada[1], M.Iwahara[1] and S.C.Mukhopadhyay[2]
[1]*Kanazawa University, 2-40-20 Kodatsuno, Kanazawa,Japan*
[2]*Massey University, Palmertston North, New zealand*
dhirasak@yahoo.com

Abstract

We present an eddy-current test (ECT) method for detecting conductive microbeads on a non-conductive substrate. A Helmholtz coil is used to generate an exciting magnetic field. The magnetic fields, generated by eddy-currents in a Pb-Sn microbead, are detected by a spin-valve giant magnetoresistive (SV-GMR) sensor. The experimental results are compared to an analytical solution for the magnetic field over the microbead. Early results for the detection of a grid of microbeads are also presented.

Keywords: conductive microbead, eddy-current testing, spin-valve giant magnetoresistance, Helmholtz coil.

1. Introduction

Eddy-current testing (ECT) is an effective way of detecting cracks and corrosion in conductive materials. It is an inexpensive, non-invasive and non-destructive inspection technique that is widely used in the aviation, nuclear power and automotive industries.

It is also commercially important to detect flaws in small conductive structures such as the tracks of a PCB, and to detect small conductive objects such as solder microbeads (see figure 1). Solder microbeads are increasingly used in the electronics industry as a way of mounting very small packages on a substrate.

In recent years new forms of ECT have been reported. An ECT type based on a meander coil exciter and a spin-valve GMR sensor was developed by [1, 2]. Using this method it was possible to detect flaws in circuit board tracks. However the coil and sensor geometry placed many restrictions on the sensitivity of detection. In particular the coil and sensor had to be placed very close to the detected object.

Please refer to Figure 2. In this paper we present an ECT probe consisting of a pair of coils in the Helmholtz arrangement, with one above (A) and one below (B) the specimen, and a SV-GMR sensor (C) placed between the coils and near the specimen (D). Conductive microbeads of radius 125-250 μm on a non-conductive surface were detected.[1] An analytical model and a Finite Element Method of the detection method are developed and are compared to experimental results.

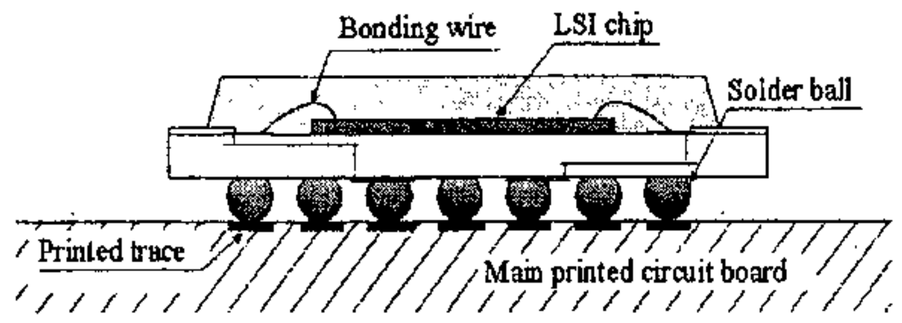

Fig 1. A ball-grid array package is connected to a PCB by an array of conductive (solder) microbeads.

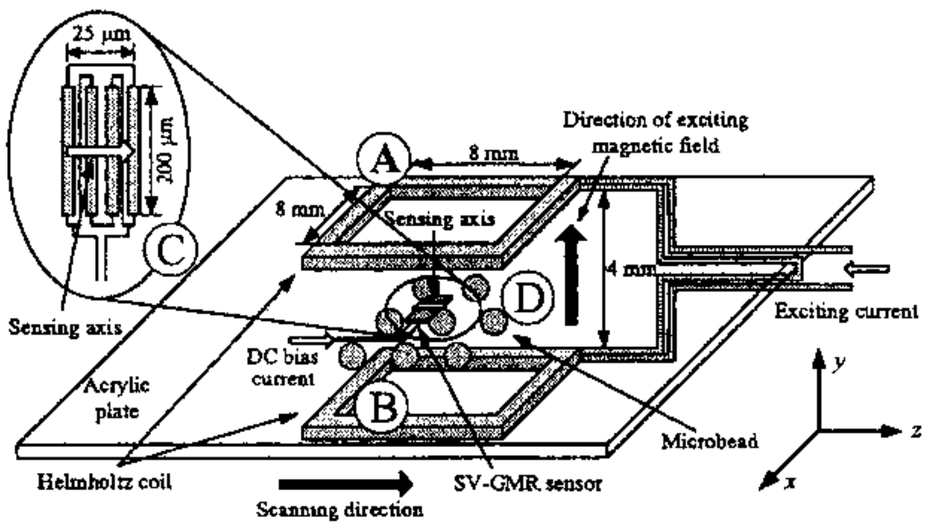

Fig 2. ECT probe structure with conductive microbeads (PbSn)

2. Detection of a Microbead by Helmholtz Technique

The increasing demand for miniaturized electronic devices has driven the development of very compact package types for integrated circuits. To achieve extreme miniaturization the contacts on the package have to be made small and close together. The Ball grid array (BGA) package achieves this by having an array of small contacts on the underside that mate with solder microbeads on the surface of a PCB. The arrangement is shown schematically in Figure 1. BGA-package ICs are available with various pad diameters. 1.0 mm diameter pads are common; the smallest currently available are about 100 μm.

If any connector on any component on a PCB fails to join to the PCB during soldering, it is likely to cause incorrect functioning of the circuit. When older, large-scale IC packages are used, it is sometimes economical to manually check and correct bad solder joints. However with the modern BGA package types, most of the solder joints are under the package where they cannot readily be seen or changed. A failed solder joint on such a package can mean that a whole PCB is rejected.

A common reason for a failed solder joint under a BGA package is an incorrect volume of solder on a PCB contact. Various methods have been developed to check the dimensions of the solder microbeads before components are attached. One method is to take a digital micrograph of the solder beads and use image processing to determine if any PCB contact is "dry" [3,4].

Here we will present an ECT method for the quality control of solder microbeads, based on a square Helmholtz coil exciter and an SV-GMR detector. The square Helmholtz coil generates an AC magnetic field which passes through the conductive microbead and generates eddy currents in the metal. The SV-GMR sensor is aligned so as to be insensitive to the Helmholtz coil field, and can thus detect the very small magnetic field which is generated by the eddy current in the microbead.

2.1 Experimental apparatus

The apparatus consisted of a Helmholtz coil pair and an SV-GMR sensor. The coils were of copper and had a square form with side length 8 mm. The upper coil and lower coil were connected in series. An AC exciting current of 200 mA was passed through the coils to generate the magnetic field. In this work two exciting frequencies were used: 5 MHz and 10 MHz. The y direction of the coordinate system used in this work was defined as the direction of the magnetic field, with the upward direction arbitrarily the positive sense.

The SV-GMR sensor had a thickness of 50 μm and an effective area of 25 μm x 200 μm. The sensor had a protective polymer cover of thickness 30 μm. As shown in Figure 2, the sensitive axis of the sensor was at right angles to the magnetic field, that is, at right angles to y, and was defined to be the z direction. The long axis of the sensor was also at right angles to the magnetic field and was defined to be the z direction. The lower face of the sensor, meaning the lower face of the protective polymer package of the sensor, was placed slightly above the plane of the highest point on the specimen.

The Helmholtz coil pair and SV-GMR sensor were mounted in an acrylic frame that moved as one rigid body. This assembly was scanned over the surface of the specimen area using a two-axis stage controller. The position resolution of the scanner was 20 μm. The scan

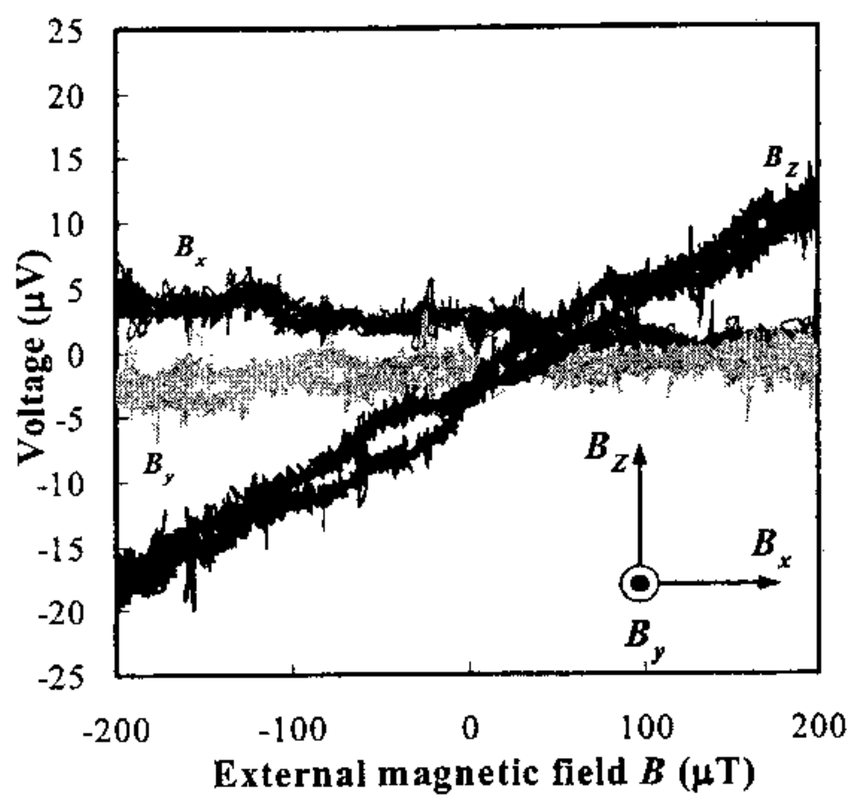

Fig 3. SV-GMR characteristics in each direction at frequency of 10 kHz

plane was the x-z plane using the coordinates defined above.

Several specimen arrangements were studied. In all experiments the microbead material was Pb-Sn solder. For the first experiments a single microbead was used. In the single-microbead experiments four radiuses were tested (125 μm, 150 μm, 200 μm and 250 μm). In later tests a grid of four by four 125 μm beads were used and the beads were laid out on a square grid with average pitch 480 μm.

2.2 Characteristics of the SV-GMR

The SV-GMR sensor was designed to have a most-sensitive direction. However some response was also expected for magnetic fields at right angles to this direction. To evaluate this, the sensor was placed between the Helmholtz coils but in three different orientations: with the sensitive direction aligned with the global x, y and z directions. The magnetic field for these tests was driven at 10 kHz and with strength 400 μT peak-to-peak.

The SV-GMR sensor was biased with a constant current of 2.5 mA. A lock-in amplifier was used to measure the voltage difference across the terminals of the SV-GMR sensor. The lock-in amplifier timing signal was derived from the power amplifier for the Helmholtz coils. Figure 3 shows the response of the sensor. It will be seen that the sensitive direction responded at about 72 μV/mT and that this response was greater than for the other two directions (15 μV/mT).

The resistance of the GMR sensor, in the absence of an applied magnetic field, was about 1.9 kΩ. The conductivity of the copper Helmholtz coil wire was

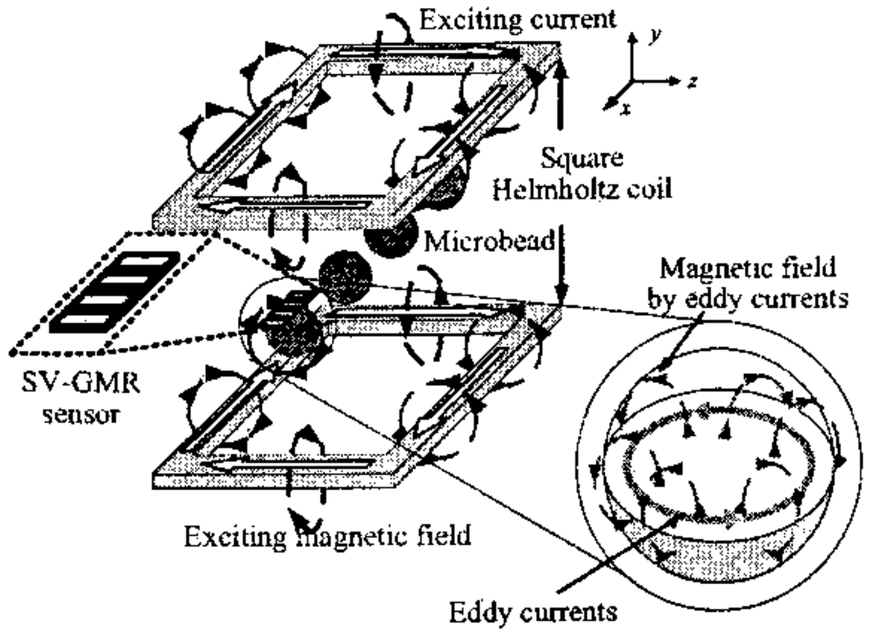

Fig 4. Arrangement of the ECT probe and conductive microbead

5.76×10^7 S/m and the conductivity of the solder microbead material was 6.8×10^6 S/m [5].

2.3 Detection Principle

Figure 4 shows the principle of microbead detection. A sinusoidal current with frequency 5 MHz is applied to the square Helmholtz coil. The square coil form was chosen because it produces a reasonably homogenous and straight magnetic field which is normal to the planes of the coils [6] . Figure 4 is drawn for an instant when the current happens to be flowing clockwise around the loops. The coils generate an AC magnetic field which induces an eddy current in the conductive microbead. Observe that the direction of the eddy current in the bead opposes that in the exciting coil. The eddy current in the microbead generates a small magnetic field as shown.

The detection approach was to measure the z-axis component of the magnetic field generated by the microbead eddy currents.

2.4 Investigation of the magnetic field distribution between the Helmholtz coils using FEM

The experimental apparatus described above was designed to produce a homogenous magnetic field near the specimen and SV-GMR sensor. An FEM model was used to check that this was achieved. The model parameters included exciting current 200 mA at 5 MHz, and the simulated specimen was a single microbead with radius 125 μm. The physical arrangement of the model elements simulated the real equipment as described above. Maxwell® 3D software version 10 from Ansoft Corporation. was used [7].

Figure 5 shows a plot of the magnitude of the magnetic field vector as calculated by the Maxwell FEM software. According to the software the field is quite smooth near the centre of the coils.

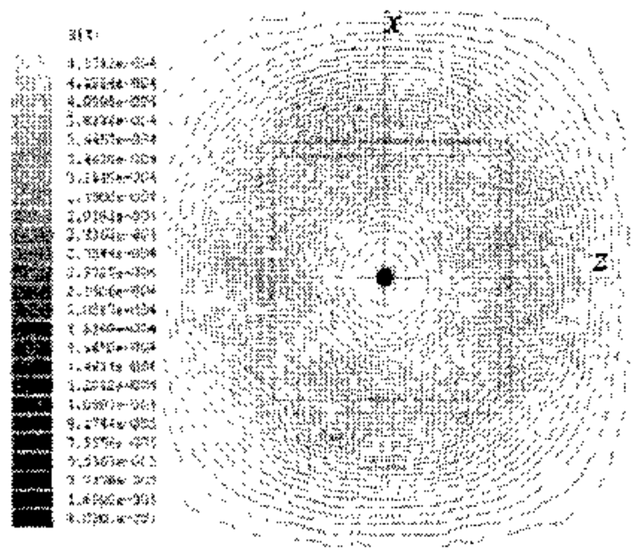

Fig 5. Magnetic field magnitude distribution as calculated by FEM.

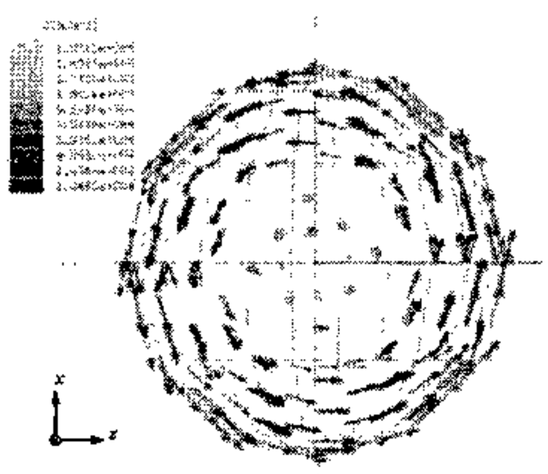

Fig 6. Eddy-current on surface of conductive microbead at 125 μm radius

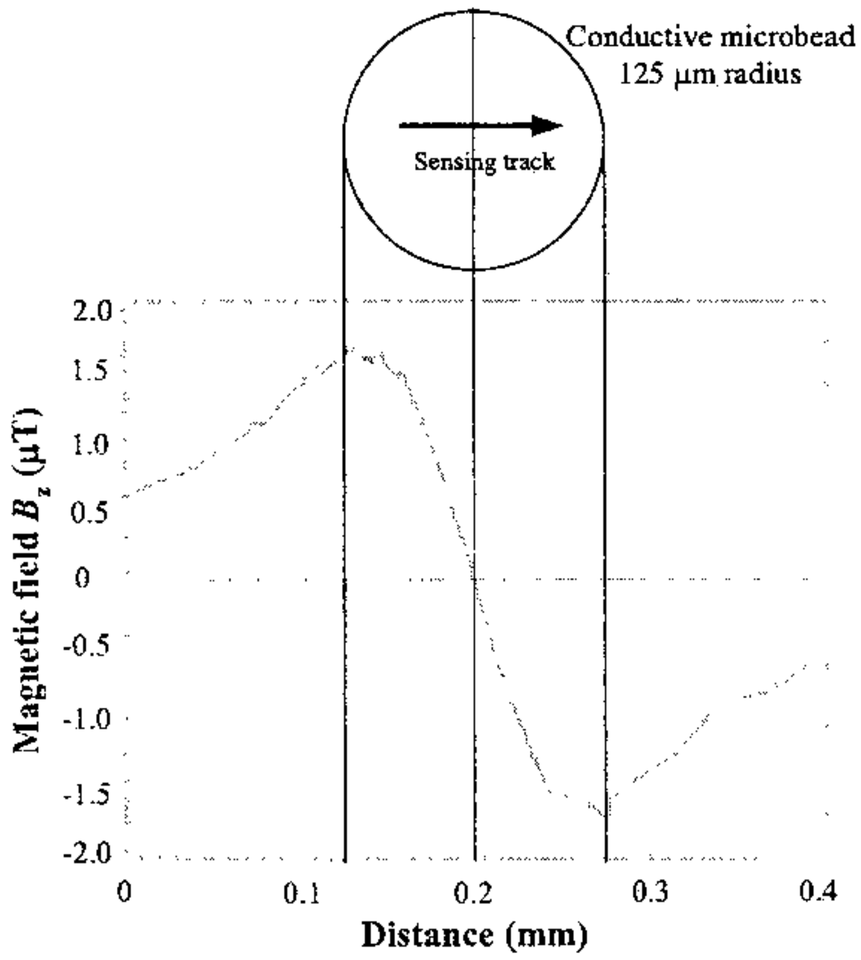

Fig 7. Magnetic field, B_z, over the sensing track obtained from FEM for a conductive microbead (PbSn) with 125 um

Figure 6 shows a plot of the eddy-current vectors inside the conductive microbead, projected on the X-Z plane, again as calculated by the software. We note that the sense of the current agrees with our expectations from Lenz's law, as explained above.

Figure 7 shows the B_z component of the magnetic field near the conductive microbead, again as estimated by the software. This plot will be revisited later when the experimental results and analytical model are compared.

3. Magnetic field model

Fig. 8 shows a simple model for the magnetic field B_z at the sensing height. The model assumes a uniform magnetic field B_0. The eddy current density inside the

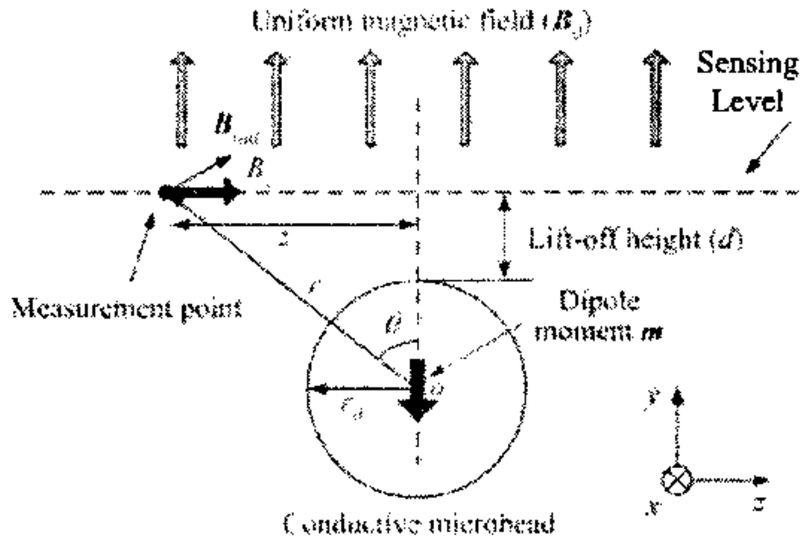

Fig 8. Analytical model

microbead, as predicted by the model, is:

$$J(r,\theta,\phi) = -j\omega\sigma a J_1(kr) B_0 \sin\theta \qquad (1)$$

where

$$a = \frac{r_0}{\mu_0} \frac{1}{J_1(kr_0)/\mu_0 + [kr_0 J_0(kr_0) - J_1(kr_0)]/\mu}$$

$$k = (-1+j)\sqrt{\omega\sigma\mu/2}$$

σ = conductivity of the microbead (6.8×10^6 S/m).
μ_0 and μ = permeability of air and the microbead.
J_0 and J_1 = zero and first order Bessel function.

It will be seen from equation 1 that the eddy-current density in the microbead is directly proportional to the frequency of the exciting magnetic field.

Manipulation of Equation (1) leads to an expression for the magnetic field density B_z at the measurement point at sensing height d:

$$B_z = 3b\frac{z(r_0+d)}{r^5} B_0 \qquad (2)$$

where

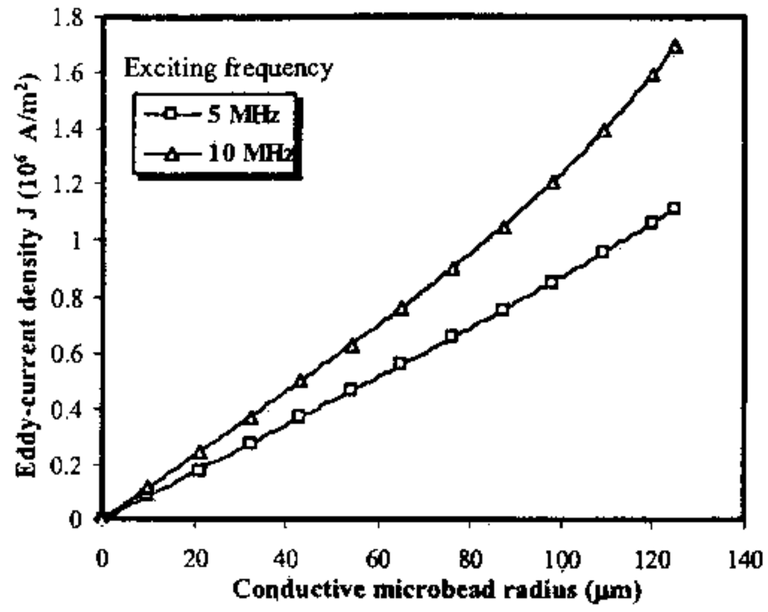

Fig 9. Eddy-current density distribution in the conductive microbead (PbSn) with the 125 μm radius

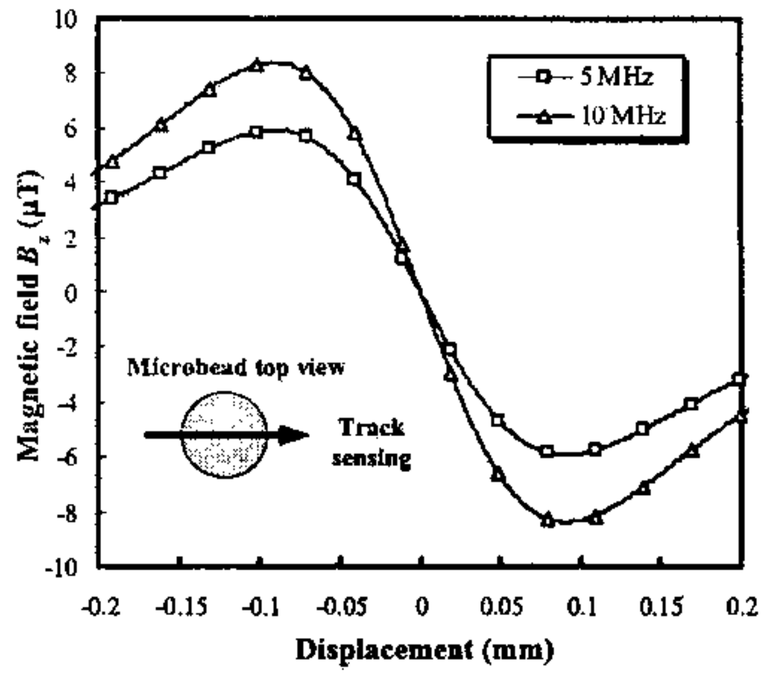

Fig 10. Magnetic field B_z over the sensing track obtained from the analytical solution for a conductive microbead (PbSn) with 125 μm radius.

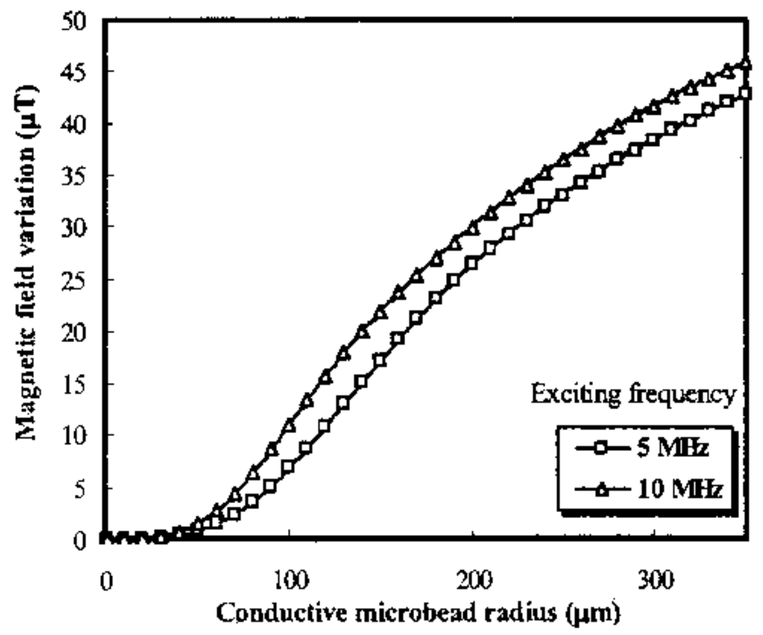

Fig 11. Maximum magnetic field variation and conductive microbead (PbSn) radius obtained from the analytical solution

$$b = r_0^3 \frac{J_1(kr_0)/2\mu_0 - [kr_0 J_0(kr_0) - J_1(kr_0)]/2\mu}{J_1(kr_0)/\mu_0 + [kr_0 J_0(kr_0) - J_1(kr_0)]/\mu}$$

In the experimental work, four different radii of microbead were used. However only one of the radii, 125 μm, was chosen for comparison to the model. In the experiments the magnetic field strength was 200 μT RMS. However in the following example of the use of the model, the field strength was set to 100 μT RMS. Inserting these values and other parameters from the experiment into equation 1, we can obtain the plots shown in Figure 9. Figures 10 and 11 shows plots of Equation 2.

4. Discussion

Three results will now be compared for the detection of a 125 μm microbead: Experimental observations, FEM results and the analytical model.

Figure 12 compares the field strength for the experiments and the models. The form of the plot for each case is quite similar, showing that the models have some predictive value.

A plot of the observed phase shift has been included on Figure 12. Interestingly it shows a sudden sign reversal near the centerline of the microbead, very like the field strength. This suggests that phase shift may also have some value in a practical system for detecting microbeads.

Figure 13 shows the effect of the microbead diameter on the strength of the measured signal, both from the analytical model and from the experiments. It will be seen that as the microbead diameter decreases, the signal tends rapidly to a low level. The general trend of the analytical and experimental plots is somewhat similar but there are also notable differences:

a) According to the analytical model, it should be possible to detect microbeads of very small radius. No experiments were performed for microbeads less than 125 μm diameter, but the trend of the plots suggests that the signal levels would be very low and perhaps not useful for detection.

b) The vertical scales for the analytical and experimental results are quite different and not really comparable. This may explain the difference in the shape in the higher diameter range.

c) The analytical model predicts higher signal strength for higher frequency excitation. However in the experiments this was not always the case. For microbeads of diameter greater than 150 μm, the *lower* frequency excitation caused a *higher* measured signal.

These differences may be attributable to non-ideal behaviour of various parts of the experimental apparatus: the power amplifier; the coils and mounting frame; and the SV-GMR sensor. Stray capacitance and other effects that increase with frequency are likely to be significant.

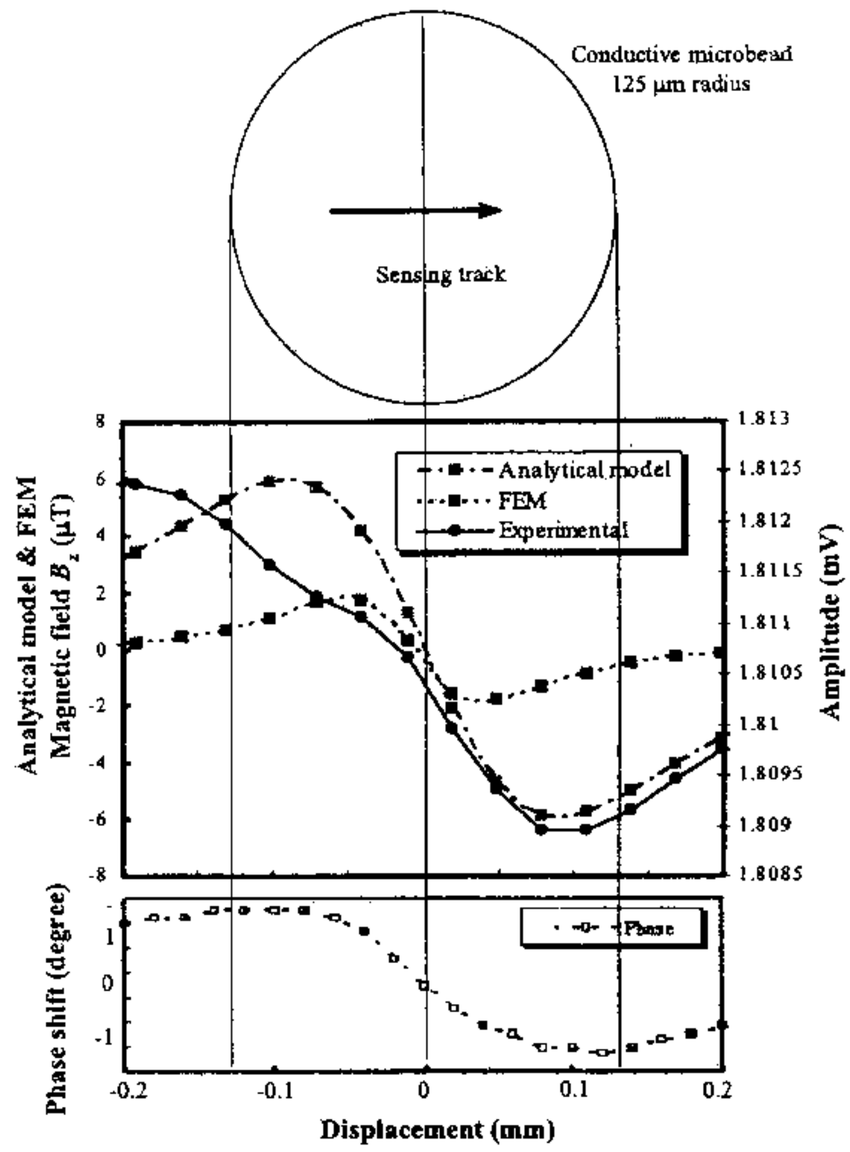

Fig 12. Comparison of FEM and analytical models with experimental results, for the case of a 125 μm microbead and exciting frequency 5 MHz.

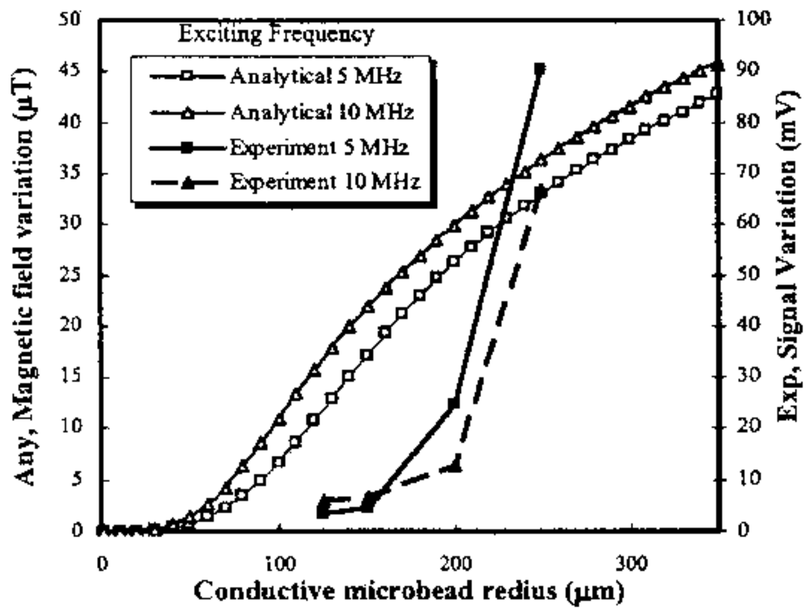

Fig 13. Amplitude of signal at the output of the lock-in amplifier, as a function of microbead diameter, and at two excitation frequencies, compared to the analytical solution

5. Extension to detection of a planar grid of microbeads

A common industrial use of conductive microbeads is in the form of a planar grid or array, for the connection to

a microchip BGA package. A typical ball grid has balls of radius 125 μm and in a square grid with pitch 400 μm. The method described above has the potential to distinguish balls in such an arrangement. An experiment was performed as follows. A grid of microbeads was made as shown in the micrograph Figure 14(a). The analytical model was applied by superimposing the solution for each microbead and this is shown in Figure 14(b). The grid was detected by the method described earlier and a filtered form of the field strength gradient is shown in Figure 14(c).

Based on the results obtained, the method described could in principle be used to detect conductive objects with radius smaller than 125 μm, depending on the properties of the sensor used.

6. Conclusion

An experimental method for the detection of conductive microbeads using a Helmholtz coil and SV-GMR sensor has been presented. The method detects the magnetic field caused by eddy currents induced in the microbeads. An FEM model and an analytical model of the phenomenon were developed and compared to the experimental results. A good level of agreement was found between experiment and the models, suggesting that the models may be used in a predictive mode within the limits of their assumptions.

An experiment to detect an array of microbeads was also performed. The analytical model for the arrangement showed good agreement with the experimental results.

7. References

[1] S. Yamada, K. Chomsuwan, Y. Fukuda, M. Iwahara, H. Wakiwaka, and S. Shoji, "Eddy-current testing probe with spin-valve type GMR sensor for printed circuit board inspection," *IEEE Trans. Magn.*, vol. 40, pp. 2676-2678, Jul. 2004.

[2] S.Yamada, K.Chomsuwan, M.Iwahara, and H.Tian, "Metallicbead detection by using eddy-current probe with SV-GMR," *Review of Progress in Quamtitative Nondestructive Evaluation*, vol 24, pp. 479-486, Jul 2004.

[3] M. Lee, M. Pecht J. Tyson and I. CMD, "Application of 3D Measurement System with CCD camera in Microelectronic," *Advanced Packaging*, pp. 33-34, November 2003.

[4] Matuura, A., Chida, A., *The engineer research magazine of Hitachi*, 21 (2002).

[5] William H.Hayt, Jr., Engineering Electromagnetics 5th ed., Singapore: McGraw-Hill, 1989

[6] M.Martin, "Equation for the Magnetic field Produced by One or More Rectangular Loops of Wire in the same Plane," *Journal of Research of the National Institute of Standards and Technology*, vol 105, pp. 557-564, Jul - Aug 2001

[7] Ansoft Corporation., Maxwell 3D software version 10.0, 2003

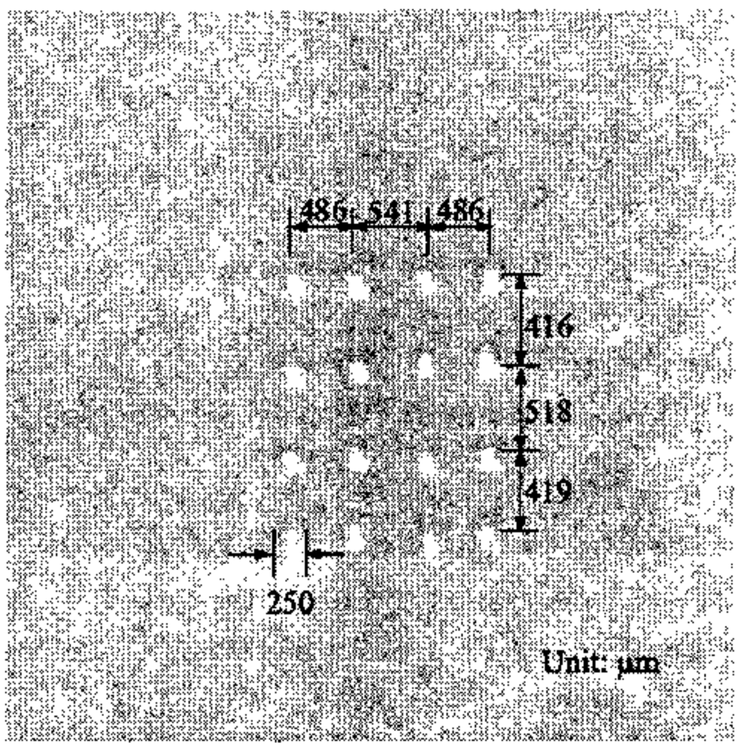

(a) Model of ball grid array

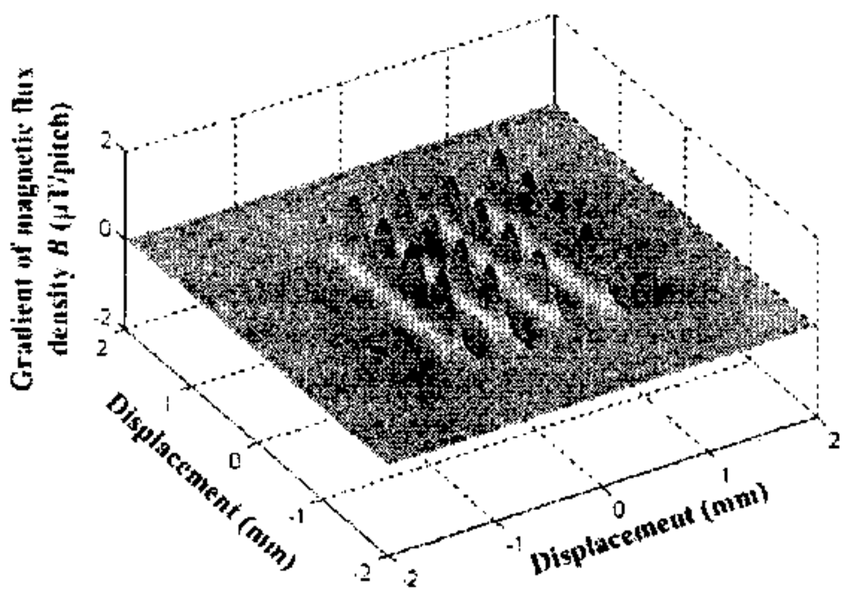

(b) Analytical result

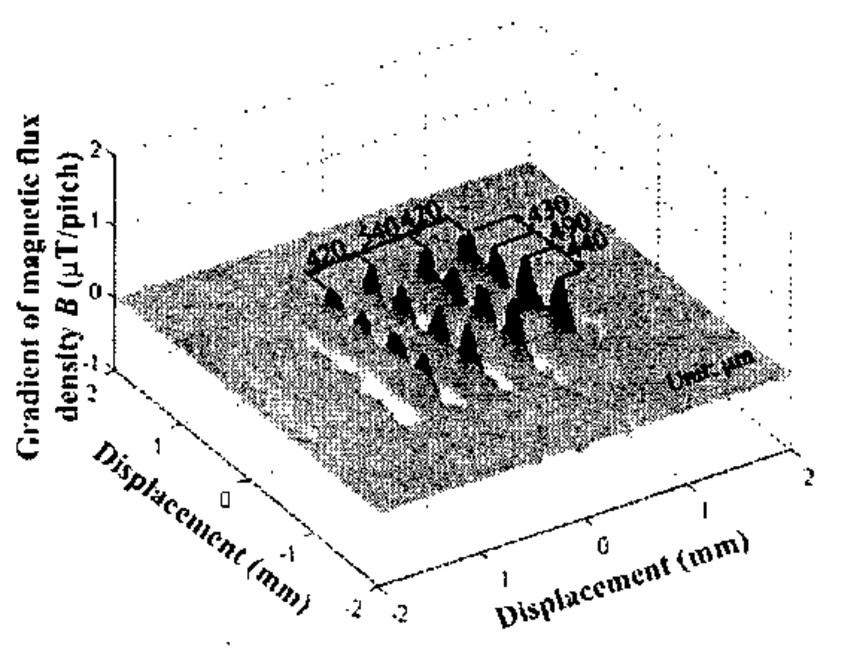

(c) Experimental result

Fig 14. Analytical and experimental results for detection of a grid of conductive microbeads.